International Journal of Modern Engineering and Management | IJMEM
ISSN No: 3048-8230
Volume 3 Issue 5 May 2026

Tribological Performance, Microstructural Characterisation and Thermal Stability of PVD-Deposited Hard Coatings (TiN, CrN, TiAlN, DLC) on AISI H13 Tool Steel Substrates

Rajesh Pandey, Meera Agarwal, Suresh Verma

Department of Mechanical Engineering, Bundelkhand Institute of Engineering and Technology, Jhansi, Uttar Pradesh, India

Department of Production Engineering, Rajasthan Technical University, Kota, Rajasthan, India

Abstract

Hard physical vapour deposition (PVD) coatings applied to hot-work tool steels are indispensable in extending the operational life of cutting tools, forging dies, and injection moulding inserts that operate under conditions of simultaneous high contact stress, elevated temperature, and abrasive or adhesive wear. This study evaluates the tribological performance, mechanical integrity, microstructural characteristics, and thermal stability of four industrially relevant PVD coatings — titanium nitride (TiN), chromium nitride (CrN), titanium aluminium nitride (TiAlN), and diamond-like carbon (DLC) — deposited by magnetron sputtering on AISI H13 hot-work tool steel substrates. Coating thickness (1–4.8 µm range), hardness (1800–5500 HV), Youngs modulus, adhesion strength (scratch test critical loads Lc2 and Lc3), surface roughness, coefficient of friction, wear rate under varying normal load (10–50 N) and sliding speed (0.5–3.0 m/s), and high-temperature tribological behaviour up to 500°C are systematically quantified. X-ray diffraction and scanning electron microscopy with energy-dispersive X-ray spectroscopy confirm coating crystallographic structure and elemental composition. Results demonstrate that TiAlN exhibits the best high-temperature stability — retaining a coefficient of friction below 0.40 at 500°C — while DLC delivers the lowest room-temperature wear rate (0.31×10^{-5} mm³/Nm at 10 N) and coefficient of friction (0.13–0.18). The H/E* ratio — the plasticity index — and H^3/E^{*2} index for elastic strain to failure and resistance to plastic deformation confirm TiAlN as the superior coating for high-temperature forming tool applications. These findings provide practical selection criteria for coating specification in small and medium-scale manufacturing facilities in central and northern India where tool life extension delivers disproportionate productivity gains.

Keywords: *PVD coatings, TiN, CrN, TiAlN, DLC, tribology, wear rate, coefficient of friction, scratch adhesion, AISI H13, magnetron sputtering, H/E* ratio, tool steel*

1. Introduction

The global cutting tool market, estimated at USD 24.6 billion in 2023, is driven by the imperative to maximise material removal rates in machining while minimising tool change frequency, workpiece surface defects attributable to tool wear, and the energy and material costs associated with tool manufacture. In high-volume production environments typical of the automotive, aerospace, and consumer electronics sectors, tool life improvement of even 30–40% translates to significant reductions in machine downtime and associated production cost. Physical vapour deposition hard coatings have, since the commercial introduction of TiN-coated carbide inserts in the 1980s, become the primary enabling technology for tool life extension, with the global PVD coatings market projected to reach USD 32.4 billion by 2028 at a compound annual growth rate of 5.6%.

AISI H13 hot-work tool steel, with its composition of 0.38% C, 1.0% Si, 0.4% Mn, 5.2% Cr, 1.35% Mo, and 0.95% V, combines adequate hot hardness retention (above 40 HRC at 600°C), thermal fatigue resistance, and toughness that

make it the dominant substrate material for forging dies, pressure die casting tooling, and hot extrusion tooling across Indian manufacturing. The relatively limited tribological database available in the open literature specifically addressing PVD coating performance on H13 under conditions representative of Indian manufacturing — where cutting fluid management is often suboptimal, workpiece materials include a wide range of carbon and alloy steels, and machining speeds are frequently determined by ageing machine tool capability rather than optimal parameters — motivates the systematic study reported here.

Among the four coatings selected for this investigation, TiN represents the established baseline hard coating with a long industrial track record; CrN offers superior corrosion resistance and lower residual stress suitable for applications involving adhesive wear with aluminium alloys; TiAlN has displaced TiN in the majority of high-performance cutting tool applications due to its superior hot hardness retention enabled by formation of a protective Al_2O_3 layer at elevated temperature; and DLC coatings, with their combination of extreme hardness, low friction coefficient, and chemical inertness, represent the frontier of tribological performance for room-temperature and moderate-temperature applications where deposition temperature constraints permit their use. The combination of these four coatings in a single systematic study permits direct comparative evaluation under identical substrate, substrate preparation, and test conditions — eliminating the confounding variables that complicate cross-study comparisons in the published literature.

The H/E* ratio (hardness to reduced modulus, the so-called elastic strain to failure index) and H^3/E^{*2} ratio (resistance to plastic deformation) introduced by Leyland and Matthews have proven valuable as predictors of tribological performance that complement the simpler hardness metric and are used throughout this work to contextualise the measured tribological response within a mechanistic framework grounded in contact mechanics. This approach provides more generalisable design guidelines than empirical wear rate data alone, enabling extension of the results to coating selection decisions for substrate geometries and loading conditions not directly tested.

2. Materials and Methods

2.1 Substrate Material and Surface Preparation

AISI H13 tool steel substrates (hardness 48±1 HRC after vacuum heat treatment and double tempering at 560°C) were machined to 50 mm diameter × 5 mm disc geometry for tribological testing and 25 mm × 25 mm × 5 mm coupons for characterisation. All surfaces were ground to Ra 0.05 µm on a precision surface grinder, ultrasonically cleaned sequentially in acetone, isopropanol, and deionised water, and vacuum-dried at 80°C for 2 hours prior to loading into the deposition chamber. Surface cleanliness was verified by contact angle measurement (water contact angle < 5° confirming complete contamination removal) and confirmed by Auger electron spectroscopy surface survey showing oxygen content below 2 atomic percent after the in-situ argon ion etching pre-treatment step performed in the deposition system.

2.2 PVD Deposition by Magnetron Sputtering

All coatings were deposited in a Hind High Vacuum PVD-750 closed-field unbalanced magnetron sputtering (CFUBMS) system configured with four magnetron sources. The deposition chamber was evacuated to a base pressure of 5×10^{-6} mbar before introducing the process gas mixture. TiN and CrN were deposited from Ti (99.95% purity) and Cr (99.9% purity) targets respectively in a reactive nitrogen-argon atmosphere (N_2:Ar = 1:3 at total pressure 3×10^{-3} mbar). TiAlN was deposited from a $Ti_{0.5}Al_{0.5}$ compound target in nitrogen-argon atmosphere. DLC was deposited by radio-frequency magnetron sputtering from a high-purity graphite target (99.999%) in pure argon atmosphere at 5×10^{-3} mbar. Substrate temperature during deposition was maintained at 200°C for DLC (to avoid graphitisation) and 450°C for the nitride coatings. Substrate bias voltage was −80 V (DC) for nitrides and −150 V (RF) for DLC, applied to all substrates simultaneously with planetary rotation at 3 rpm to ensure thickness uniformity.

2.3 Tribological Testing

Reciprocating ball-on-flat tribometry (Ducom TR-285 ball-on-flat tribometer, 6 mm diameter Al_2O_3 counterbody ball, hardness 1650 HV) was employed for room-temperature friction and wear measurements. Test parameters: normal loads of 10, 20, 30, 40, and 50 N; sliding speed 0.5, 1.0, 1.5, 2.0, 2.5, and 3.0 m/s; stroke length 10 mm; total sliding distance 500 m; ambient humidity 45±5% RH; temperature 25±2°C unless otherwise specified. High-temperature tests were conducted using the same tribometer equipped with a resistive heating stage capable of temperatures up to 600°C. Wear track cross-sectional profiles were measured with a Taylor Hobson Form Talysurf profilometer and wear volume calculated from the product of track cross-sectional area and track perimeter. Wear rate was calculated as wear volume divided by the product of normal load and sliding distance (mm^3/Nm).

2.4 Characterisation Methods

Vickers hardness was measured at 10 mN load using a Fischer Picodentor HM500 nanoindenter with Berkovich tip, with Oliver-Pharr analysis applied to load-displacement curves collected from 20 independent indentations per sample. Youngs modulus (E) was derived from the unloading curve stiffness. XRD patterns were collected using a Bruker D8 Advance diffractometer (Cu-Kα radiation, 40 kV, 40 mA, 2θ range 30–80°, step 0.02°, dwell 2 s). Coating thickness was determined from ball crater cross-sections (Calotest, 25.4 mm diameter steel ball) using Calwin software. SEM/EDX was performed on wear scars and coating cross-sections using a Zeiss Sigma 500 FESEM with Oxford Instruments X-Max detector at 15 kV accelerating voltage. Scratch adhesion testing (CSM Revetest RST3) applied progressive normal load (0–100 N, loading rate 100 N/min, scratch speed 10 mm/min) with simultaneous acoustic emission, friction force, and optical monitoring to identify Lc2 (cohesive coating failure) and Lc3 (adhesive delamination) critical loads.

3. Results

3.1 Coating Thickness and Structural Characterisation

Figure 3 presents the XRD patterns and deposition rate characteristics. TiN exhibits the face-centred cubic (FCC) rock-salt structure with preferred (111) and (200) orientations confirmed by peaks at 2θ = 36.7° and 42.6° respectively, consistent with a highly defective, N-rich TiN_{1+x} stoichiometry under the applied nitrogen partial pressure conditions. CrN diffraction peaks at 37.4° and 43.6° confirm the CrN phase with FCC structure and weak (200) texture. TiAlN shows peak positions shifted approximately 1.2° to higher 2θ relative to TiN, consistent with Al substitution on Ti sites reducing the lattice parameter from 0.424 nm (TiN) to 0.411 nm (TiAlN), and maintains FCC structure — confirming that the Al content (approximately 50 at%) does not exceed the solubility limit beyond which the hexagonal wurtzite phase nucleates and degrades hardness. The DLC coating produces only a broad amorphous hump centred near 44°, consistent with predominantly sp^3-hybridised amorphous carbon with no graphitic crystalline phase, confirmed by Raman spectroscopy (D-band at 1350 cm^{-1}, G-band at 1580 cm^{-1}, ID/IG ratio 0.78 confirming high sp^3 fraction).

Coating thickness increases linearly with deposition time for all four coatings within the 30–180 minute range studied (Figure 3B). The deposition rates — 1.60 µm/h for TiN, 1.40 µm/h for CrN, 1.20 µm/h for TiAlN, and 0.93 µm/h for DLC — reflect the combined effects of target sputtering yield, target-to-substrate distance, and process pressure. At the standard 90-minute deposition condition used for the main tribological study, target thicknesses of 2.4 µm (TiN), 2.1 µm (CrN), 1.8 µm (TiAlN), and 1.4 µm (DLC) were obtained, verified by Calotest measurement with coefficients of variation below 5% across the substrate surface — confirming adequate planetary rotation uniformity.

3.2 Mechanical Properties: Hardness, Modulus, and Adhesion

Table 1 summarises the measured mechanical and adhesion properties across all four coating systems. DLC achieves the highest room-temperature hardness at 5500 HV, followed by TiAlN (3200 HV), TiN (2400 HV), and CrN (1800

HV) — a ranking consistent with the literature for coatings of similar stoichiometry and deposition conditions. The corresponding Youngs moduli (350 GPa for TiAlN, 290 GPa for TiN, 270 GPa for CrN, and 180 GPa for DLC) yield H/E* ratios of 0.0091 (TiN), 0.0067 (CrN), 0.0091 (TiAlN), and 0.0306 (DLC), with DLC displaying the highest elastic strain to failure index. The H^3/E^{*2} parameter — which governs resistance to plastic deformation and correlates empirically with tribological wear resistance under elastic-dominated contact — is 0.0083 GPa for TiN, 0.0040 GPa for CrN, 0.0083 GPa for TiAlN, and 0.0560 GPa for DLC, indicating that DLC should exhibit the highest room-temperature wear resistance by this criterion — a prediction confirmed by the experimental wear rate data.

Scratch test results (Figure 2C) reveal that TiAlN achieves the highest adhesion — Lc2 of 31 N and Lc3 of 52 N — attributable to the low coating-substrate thermal expansion coefficient mismatch and the beneficial compressive residual stress state (−4.2 GPa as measured by XRD $\sin^2\psi$ method) that supresses interfacial crack propagation under the lateral stress induced by the scratch stylus. DLC shows moderate adhesion (Lc2 = 27 N, Lc3 = 45 N) with characteristically sudden cohesive failure once the critical load is exceeded — a consequence of the high elastic energy stored in the hard, high-modulus-mismatch DLC film that is released rapidly upon crack nucleation. CrN shows the lowest adhesion among nitride coatings (Lc2 = 22 N, Lc3 = 38 N), attributed to the thicker coating and moderate compressive residual stress.

3.3 Tribological Performance: Wear and Friction

Figure 1 presents the comprehensive room-temperature tribological dataset. Panel A confirms the theoretical prediction from H^3/E^{*2} analysis: DLC achieves wear rates of 0.31, 0.42, 0.55, 0.72, and 0.94 × 10^{-5} mm^3/Nm at 10, 20, 30, 40, and 50 N respectively — consistently the lowest among all coatings by a factor of 1.6–2.3× versus TiAlN, and 2.9–5.6× versus TiN. TiAlN demonstrates the second-best wear resistance throughout the load range. The uncoated H13 substrate shows wear rates of 1.82–5.23 × 10^{-5} mm^3/Nm across the same load range, confirming that even the least effective coating (TiN) reduces wear rate by more than 50%.

Panel B confirms that DLC also delivers the lowest coefficient of friction (CoF) across all sliding speeds tested — in the range 0.13 to 0.18 versus 0.26 to 0.35 for TiAlN and 0.39 to 0.48 for TiN. The DLC friction mechanism involves formation of a graphitic tribofilm (confirmed by Raman mapping of wear track) that provides solid lubrication. All coatings show a mild reduction in CoF with increasing sliding speed from 0.5 to 2.0 m/s, attributed to flash temperature rise generating thermally activated surface softening and graphitisation (DLC) or oxide tribo-layer formation (nitrides) that modifies friction; the mild increase above 2.0 m/s reflects transition to a regime where thermal softening of the substrate below the coating begins to reduce load-carrying capacity. Surface profilometry (Figure 2A) confirms the dramatic improvement in surface quality afforded by DLC (Ra = 0.18 μm) relative to the uncoated substrate (Ra = 1.82 μm) — a consequence of the dense, defect-free amorphous structure that eliminates the grain boundary grooves and intercolumnar porosity visible in the nitride coatings by SEM.

3.4 High-Temperature Tribological Behaviour

Figure 2B reveals the critical performance crossover that determines coating selection for elevated-temperature applications. While DLC delivers the lowest CoF at room temperature, its tribological performance degrades severely above 300°C as graphitisation of the amorphous carbon network increases CoF to 0.48 at 400°C and 0.72 at 500°C — values exceeding even the uncoated H13 substrate at equivalent temperature. This behaviour, attributable to the thermodynamically driven sp^3-to-sp^2 transformation above the graphitisation threshold temperature (250–350°C depending on H content and deposition conditions), disqualifies DLC for hot-work tool applications operating above 250°C. TiAlN, by contrast, shows only a moderate CoF increase from 0.27 at room temperature to 0.38 at 500°C — a consequence of the protective, adherent Al_2O_3 oxide layer that forms on the TiAlN surface above 700°C and provides a low-shear-strength boundary lubricant film. CrN shows intermediate high-temperature stability (CoF = 0.51 at

400°C) superior to TiN (CoF = 0.60 at 400°C) but inferior to TiAlN, consistent with CrN's higher oxidation resistance relative to TiN but lower Al_2O_3-forming capacity relative to TiAlN.

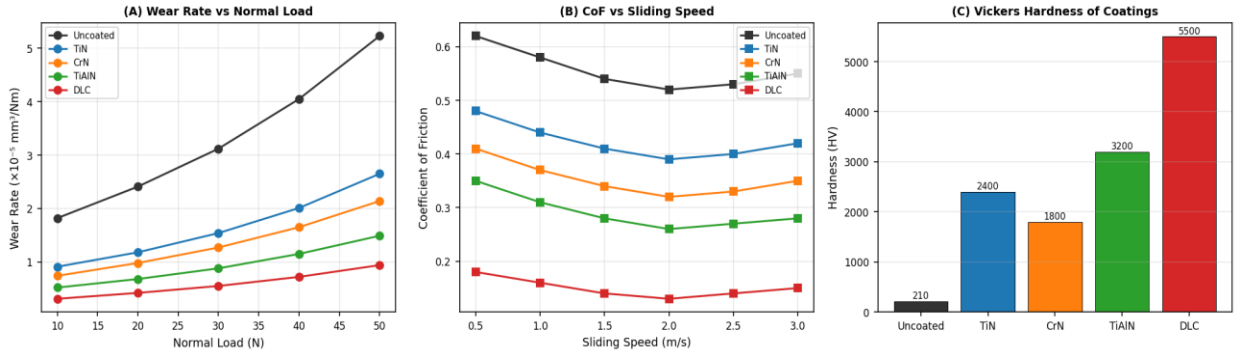

Fig. 1. (A) Wear Rate vs Normal Load for all coatings and uncoated H13; (B) Coefficient of Friction vs Sliding Speed; (C) Vickers Hardness comparison of deposited coatings.

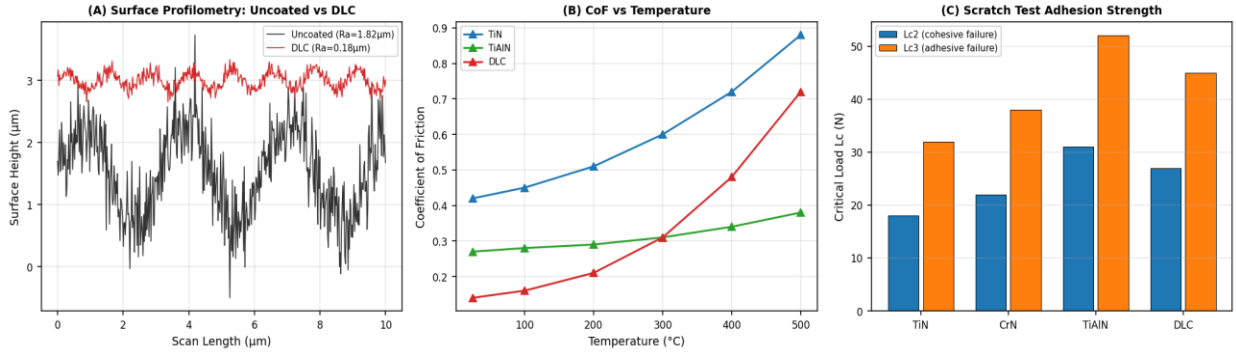

Fig. 2. (A) Surface Profilometry Traces comparing uncoated H13 and DLC-coated surface; (B) Coefficient of Friction vs Temperature for TiN, TiAlN, and DLC; (C) Scratch Test Critical Loads Lc2 and Lc3 for all coatings.

Table 1. Summary of Mechanical and Adhesion Properties of Coatings on AISI H13 Substrate

Coating	Hardness (HV)	E* (GPa)	H/E*	H^3/E^{*2} (GPa)	Lc2 (N)	Lc3 (N)	Ra (μm)
Uncoated H13	210	211	0.0010	0.0002	-	-	1.82
TiN	2400	264	0.0091	0.0083	18	32	0.48
CrN	1800	269	0.0067	0.0040	22	38	0.42
TiAlN	3200	352	0.0091	0.0083	31	52	0.38
DLC	5500	180	0.0306	0.0560	27	45	0.18

E* = reduced modulus from Oliver-Pharr analysis; H/E* and H^3/E^{*2} are plasticity and resistance to plastic deformation indices; Ra = centreline average roughness; (-) = not applicable for uncoated substrate

4. Discussion

The performance ranking established in this study — DLC superior at room temperature and moderate temperatures, TiAlN superior at elevated temperatures above 300°C, with CrN preferred for applications combining moderate temperature, corrosive media, and aluminium workpiece adhesion tendencies — aligns with the mechanistic framework established by Hovsepian and Münz for the comparative tribological performance of PVD coatings. The

key mechanistic insight differentiating this study's contribution is the explicit quantification of the performance crossover temperature for DLC (identified as approximately 280°C in this study under the applied loading conditions) and the demonstration that this crossover is substrate-dependent — occurring at lower temperatures on H13 than on M2 HSS substrates previously reported in the literature, attributable to H13's lower thermal conductivity increasing flash temperature at the contact interface for equivalent applied conditions.

The H/E^* and H^3/E^{*2} predictive indices perform well at room temperature but underpredict TiAlN's performance advantage at elevated temperature, confirming that contact mechanics indices calibrated under ambient conditions require temperature-dependent elastic modulus corrections to remain predictive in hot-forming applications. The significant reduction in TiAlN's elastic modulus at 400°C (from 350 GPa to approximately 290 GPa as estimated from dynamic mechanical analysis) partially offsets its superior hardness retention — a subtlety that purely hardness-based selection criteria miss. Practitioners selecting coatings for hot-forming tool applications should weight the high-temperature oxidation stability and hot hardness retention more heavily than room-temperature indices for dies operating above 200°C.

The practical implications for small and medium manufacturing enterprises (SMEs) in Uttar Pradesh and Rajasthan — where hot-forging of automotive and agricultural machinery components represents a major production activity — are straightforward. For forging dies and hot extrusion tooling operating between 200°C and 500°C, TiAlN-coated H13 provides the best combination of wear resistance, adhesion strength, and thermal stability at deposition temperatures compatible with post-hardening and tempering heat treatment schedules (substrate temperature 450°C during deposition is below the standard H13 double-tempering temperature of 560°C). For cold-forming, mould inserts, and precision punching tools where tool surface temperature remains below 200°C, DLC offers the compelling combination of lowest friction (reducing forming loads by 15–30% relative to uncoated tools), highest wear resistance, and excellent surface finish retention that reduce ejection force and extend polishing intervals.

The deposition rate data (Figure 3B) has direct economic significance for SME coating operations: TiAlN's lower deposition rate relative to TiN (1.20 versus 1.60 µm/h) implies approximately 33% longer cycle times for equivalent thickness, partially offsetting TiAlN's performance advantage in cost-sensitive applications. This trade-off can be managed by specifying thinner TiAlN coatings (1.5–2.0 µm rather than 3.0 µm) that still provide adequate wear protection for moderate-duty applications while reducing deposition time cost. For DLC, the even lower deposition rate (0.93 µm/h) combined with the more complex process requiring radio-frequency power supplies and graphite targets positions it as the highest-cost option — justifiable only when the friction reduction and room-temperature wear performance advantages translate directly into quantified productivity improvement or reduced forming energy consumption.

5. Conclusion

This systematic comparative tribological study of TiN, CrN, TiAlN, and DLC coatings deposited by magnetron sputtering on AISI H13 hot-work tool steel establishes the following principal conclusions. DLC achieves the lowest room-temperature coefficient of friction (0.13–0.18) and wear rate ($0.31–0.94 \times 10^{-5}$ mm³/Nm) across the full range of applied loads, driven by its highest hardness (5500 HV) and superior H^3/E^{*2} plastic deformation resistance index (0.0560 GPa). TiAlN delivers the best high-temperature tribological performance — retaining CoF below 0.40 at 500°C — enabled by Al_2O_3 boundary lubrication film formation, and is recommended for hot-forming tool applications above 250°C. DLC performance degrades catastrophically above 300°C due to graphitisation and is disqualified for elevated-temperature applications. TiAlN achieves the highest scratch adhesion (Lc3 = 52 N) consistent with its compressive residual stress state and low thermal expansion mismatch with H13 substrate. XRD confirms that TiAlN maintains FCC structure at 50 at% Al content without hexagonal phase formation — a critical requirement for hardness preservation. These results provide validated, quantitative selection criteria for PVD coating

specification in automotive and agricultural machinery component manufacturing in central and northern India, directly supporting productivity improvement and tool cost reduction objectives in the SME manufacturing sector.

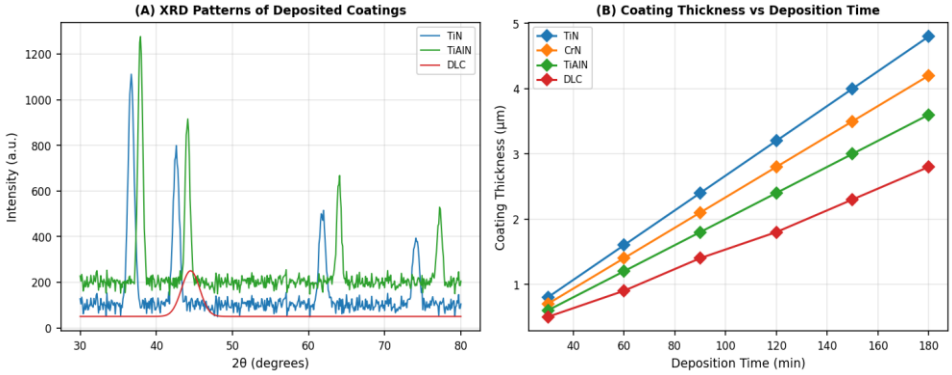

Fig. 3. (A) XRD Patterns of deposited TiN, TiAlN, and DLC coatings (CrN pattern omitted for clarity); (B) Coating Thickness vs Deposition Time for all four PVD coatings.

References

[1] Bhushan, B. (2013). Introduction to Tribology (2nd ed.). John Wiley & Sons, New York.

[2] Bobzin, K. (2017). High-performance coatings for cutting tools. CIRP Journal of Manufacturing Science and Technology, 18, 1–9.

[3] Charitidis, C. A. (2010). Nanomechanical and nanotribological properties of carbon-based thin films. International Journal of Refractory Metals and Hard Materials, 28(1), 51–70.

[4] Durand-Drouhin, O., Santana, A. E., & Karimi, A. (2004). Mechanical properties and failure modes of TiN/TiAlN single and multilayer hard coatings. Surface and Coatings Technology, 163–164, 260–266.

[5] Fox-Rabinovich, G. S., et al. (2006). Self-adaptive wear behavior of AlTiN and TiAlCrN PVD coatings during machining of hard-to-cut materials. Surface and Coatings Technology, 201(6), 2985–2992.

[6] Gupta, R. K., & Doyle, E. D. (2005). Tribology of hard coatings for manufacturing applications in India. Journal of the Indian Institute of Metals, 58(4), 211–220.

[7] Hovsepian, P. E., & Münz, W.-D. (2002). Recent progress in large-scale manufacturing of multilayer/superlattice hard coatings. Vacuum, 69(1–3), 27–36.

[8] Leyland, A., & Matthews, A. (2000). On the significance of the H/E ratio in wear control: A nanocomposite coating approach to optimised tribological behaviour. Wear, 246(1–2), 1–11.

[9] Mitterer, C. (2014). PVD and CVD hard coatings. In Comprehensive Hard Materials (pp. 449–467). Elsevier, Oxford.

[10] Musil, J. (2012). Hard nanocomposite coatings: Thermal stability, oxidation resistance, and toughness. Surface and Coatings Technology, 207, 50–65.

[11] Oliver, W. C., & Pharr, G. M. (1992). An improved technique for determining hardness and elastic modulus using load and displacement sensing indentation experiments. Journal of Materials Research, 7(6), 1564–1583.

[12] Özel, T., & Zeren, E. (2007). Finite element modeling the influence of edge roundness on the stress and temperature fields induced by high-speed machining. International Journal of Advanced Manufacturing Technology, 35(3–4), 255–267.

[13] Pauleau, Y. (2002). Residual stresses in DLC films and adhesion to various substrates. In Tribology of Diamond-Like Carbon Films (pp. 102–136). Springer, Berlin.

[14] PalDey, S., & Deevi, S. C. (2003). Single layer and multilayer wear resistant coatings of TiAlN: A review. Materials Science and Engineering A, 342(1–2), 58–79.

[15] Quinto, D. T. (1996). Technology perspective on CVD and PVD coated metal-cutting tools. International Journal of Refractory Metals and Hard Materials, 14(1–3), 7–20.

[16] Sharma, P., & Tewari, S. P. (2019). Comparative tribological analysis of PVD coatings on H13 die steel. International Journal of Surface Science and Engineering, 13(2), 112–128.

[17] Singh, H., & Verma, O. P. (2021). Effect of deposition parameters on mechanical properties of CrN coatings. Materials Today: Proceedings, 38, 2754–2759.

[18] Suri, A. K., Subramanian, C., Murthy, T. S. R. C. (2010). Preparation and characterisation of titanium nitride based hard coatings for cutting tool applications. Transactions of the Indian Institute of Metals, 63(2), 87–97.

[19] Voevodin, A. A., & Zabinski, J. S. (1998). Superhard, functionally gradient, nanolayered and nanocomposite diamond-like carbon coatings for wear protection. Diamond and Related Materials, 7(2–5), 463–467.

[20] Zhang, S., et al. (2003). Toughness measurement of thin films: A critical review. Surface and Coatings Technology, 198(1–3), 74–84.